



Evaluating SARS-CoV-2 RBD helices stability throughout the lens of molecular dynamics simulation



D. Stojanov (1), A. Velinov (1), B. Despodov (1)

1. Faculty of Computer Science, Goce Delcev University, North Macedonia

Opening

- **Study aims:** evaluate the stability of SARS-CoV-2 S-protein RBD helices.



- Five helices with variable stability rates in SARS-CoV-2 RBD.
- The most stable SARS-CoV-2 RBD helix is RBD₄₁₇₋₄₂₁=KIADY, K(Lysine) at position 417.

POSITIVE CORRELATION between

SARS-CoV-2 immune escape properties due to K417 mutations. AND RBD₄₁₇₋₄₂₁=KIADY helix destabilization.



#Experimentally
proved

Immune escape properties of SARS-CoV-2 RBD K417 mutations, Dupont et al., 2021. (K417N, K417T).

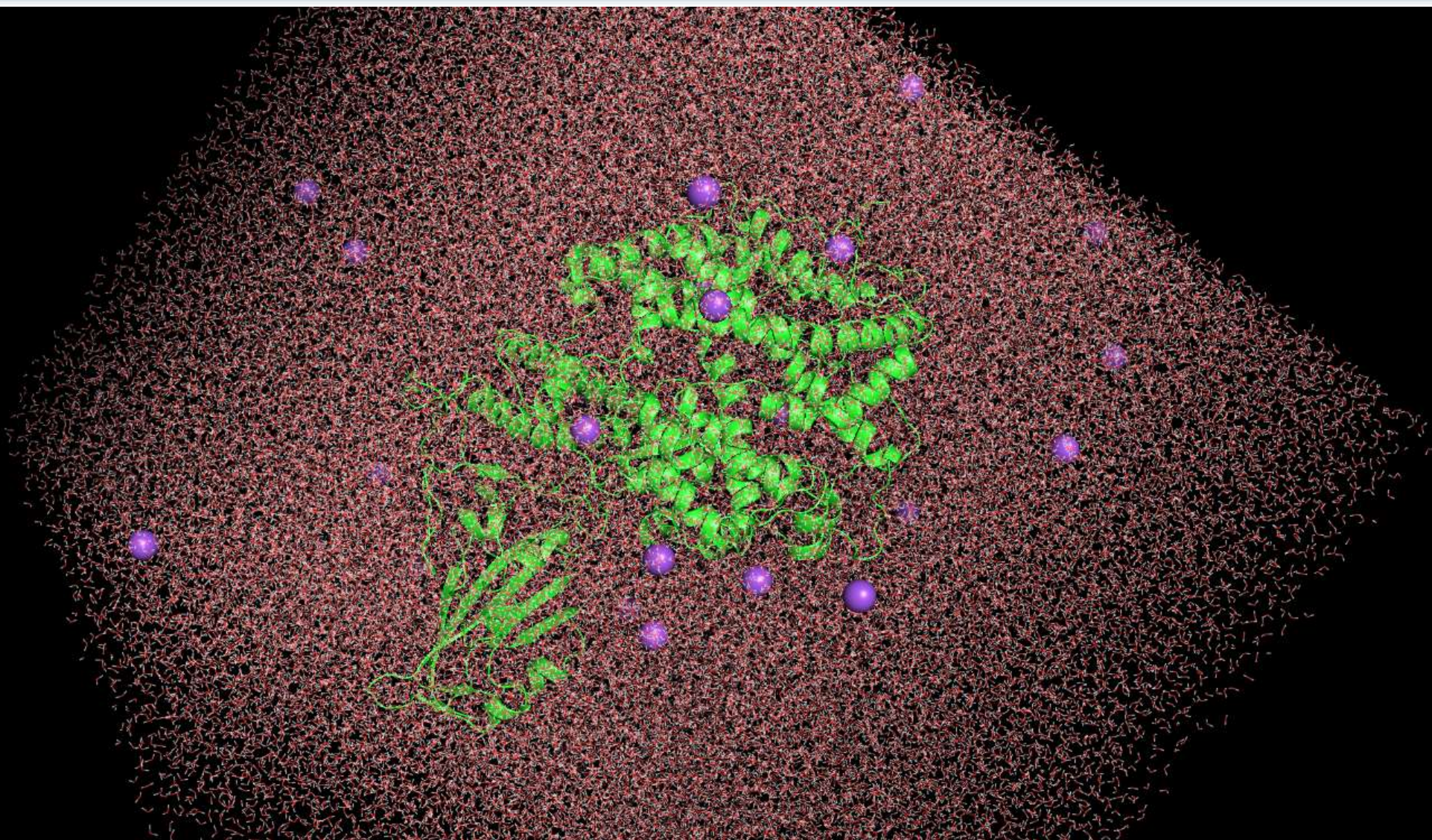
#Our findings

K417 mutations are likely to induce RBD₄₁₇₋₄₂₁=KIADY helix destabilization.

1. Experimental Settings

1. 6m0j record retrieved from the Protein Data Bank (<https://www.rcsb.org/>): “The Crystal structure of the SARS-CoV-2 spike receptor-binding domain bound with ACE2”.
2. Put the molecule in the center of a cubic solvent box (1nm x 1nm x 1nm), dissolved under the SPC/E (simple point-charge/extended) water model.
3. Brought to the neutral net charge. *The initial net charge of the system was $-25.0 e$, then changed to $0.0 e$ (neutral net charge) by substituting 25 SPC/E water molecules with 25 Na^+ ions.
4. System potential energy gradually decreased/optimized towards the plateau $-10^5 \frac{\text{kJ}}{\text{mol}}$.
5. Apply V-rescale thermostat and Berendsen barostat to bring the system up to 310 K temperature and 1 bar pressure.
6. Run 50-ns molecular dynamics simulation in Gromacs.
7. Use simulation output files for DSSP secondary structure analysis.

1. Experimental Settings

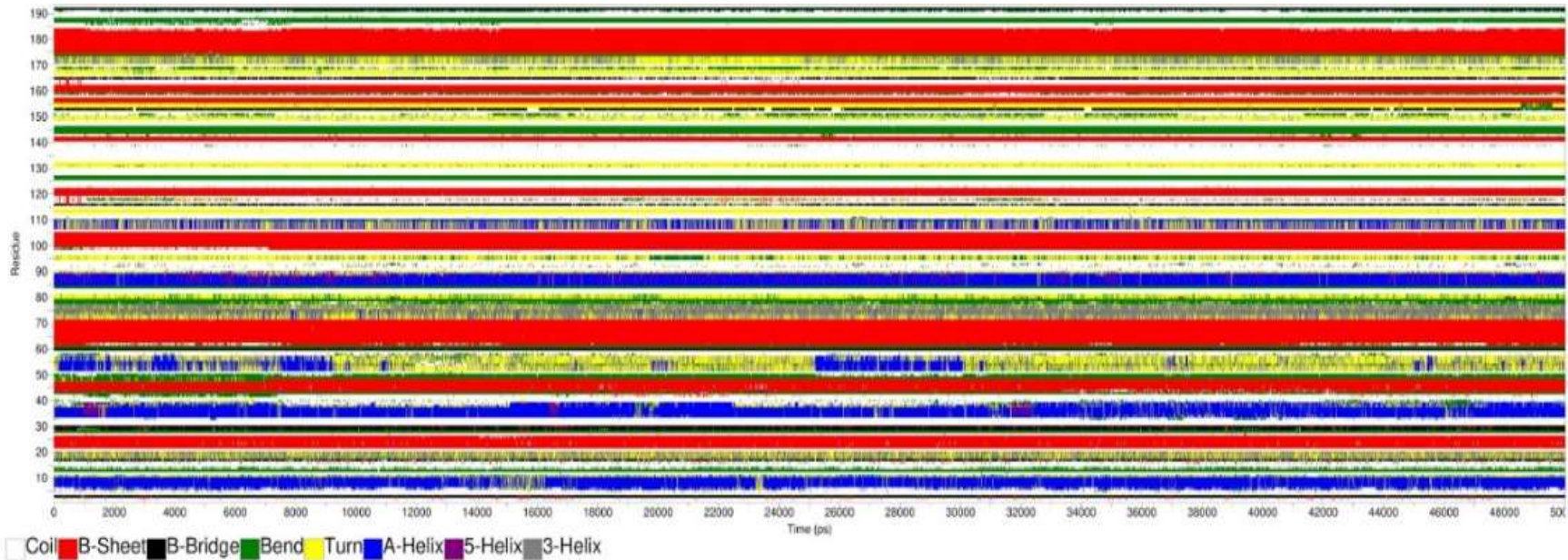


2. Dictionary of Secondary Structure in Proteins

- Per-residue assignment of the secondary structure of a protein in DSSP (Dictionary of Secondary Structure in Proteins).
- Elements prediction based on known hydrogen bonding patterns found in many secondary motifs.
- Hydrogen bond detection is based on a calculation of inter-residual electrostatic energy.
- The main chain amino group is the universal hydrogen bond donor, and the main chain oxygen atom is the universal hydrogen bond acceptor.
- $E = f q_{C,O} q_{N,H} \left(\frac{1}{r_{NO}} + \frac{1}{r_{CH}} - \frac{1}{r_{OH}} - \frac{1}{r_{CN}} \right) \left[\frac{kcal}{mol} \right]$
- $q_{C,O} = -0.42 e$ and $q_{N,H} = +0,2 e$, and $f = 332$ dimensionality constant.
- Types of secondary structure elements in DSSP:

H = alpha helix, **I** = π -helix, **G** = 3_{10} -helix, **T** = hydrogen-bonded turn, **S** = bend, **B** = β -bridge, **E** = β -sheet, **P** = kappa-helix (poly-proline II helix), \sim = loop.

3. Results



Helix	Sequence	Stability rate (%)
RBD ₃₄₀₋₃₄₃	GEVF	94.6
RBD ₃₆₆₋₃₆₉	SVLY	93.04
RBD ₃₈₄₋₃₈₉	PTKLND	23.09
RBD ₄₁₇₋₄₂₁	KIADY	98.12
RBD ₄₃₉₋₄₄₂	NNLD	57.45

4. Discussion & Concluding remarks

1. There are 3 (three) stable helices in the SARS-CoV-2 receptor-binding domain: RBD₄₁₇₋₄₂₁=KIADY (stability rate=98.12%), RBD₃₄₀₋₃₄₃=GEVF (stability rate=94.6%) and RBD₃₆₆₋₃₆₉=SVLY (stability rate=93.04%).
2. RBD₃₈₄₋₃₈₉=PTKLND holds the premise for the least stable motif (stability rate=23.09%). *Although P₃₈₄ may act as a helix breaker and K₃₈₆, and L₃₈₇ have helix-forming propensities, the last two residues in the motif N₃₈₈, and D₃₈₉ do not allow stable helix formation.
3. There is no specific secondary structure annotation of RBD₄₃₉₋₄₄₂=NNLD. *Frequent helix-to-turn oscillations are present.
 - **Key insight:** Given the current knowledge of the antigenic properties of K417 mutations and the current findings for stable RBD₄₁₇₋₄₂₁=KIADY helix formation, in addition to K417, we assume that K417 mutations may lead to RBD₄₁₇₋₄₂₁=KIADY helix destabilization – a structural change that might be associated with SARS-CoV-2 immune escape strategies.

5. Related COVID-19 Research



- **Journal:** Meta Gene, Elsevier
- **Article:** Stojanov, D. (2021). Phylogenicity of B. 1.1. 7 surface glycoprotein, novel distance function and first report of V90T missense mutation in SARS-CoV-2 surface glycoprotein.

Main findings:

- B.1.1.7 spike protein lost some of the key mutations associated to higher infectivity.
- $\Delta 168$ is supposed to compensate for missing $\Delta V70$ in B.1.1.7 spike variant.
- First report of V90T missense mutation (Spanish isolate).
- NTD mutation V90T escapes 2–51 neutralizing antibody.
- Novel formula for computing genetic distance, why not try something new instead of the old-fashioned Jaccard and Sorensen-Dice distance functions?

$$d(A, B) = \frac{|A \setminus B||A| + |B \setminus A||B|}{|A|^2 + |B|^2}$$

5. Related COVID-19 Research

- **Journal:** Biotechnology & Biotechnological Equipment, Taylor and Francis
- **Article:** Stojanov, D. (2023). Structural implications of SARS-CoV-2 Surface Glycoprotein N501Y mutation within receptor-binding domain [499-505]—computational analysis of the most frequent Asn501 polar uncharged amino acid mutations. Biotechnology & Biotechnological Equipment, 37(1), 2206492.

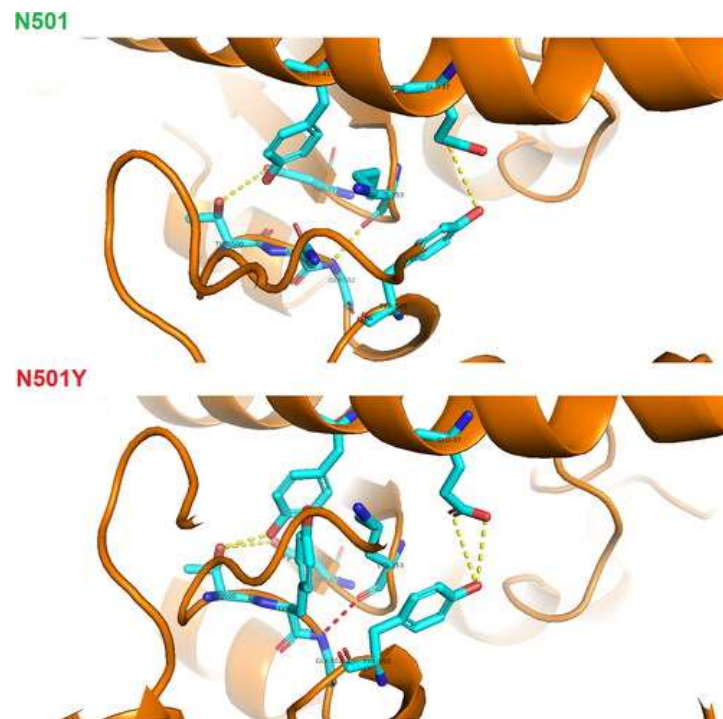
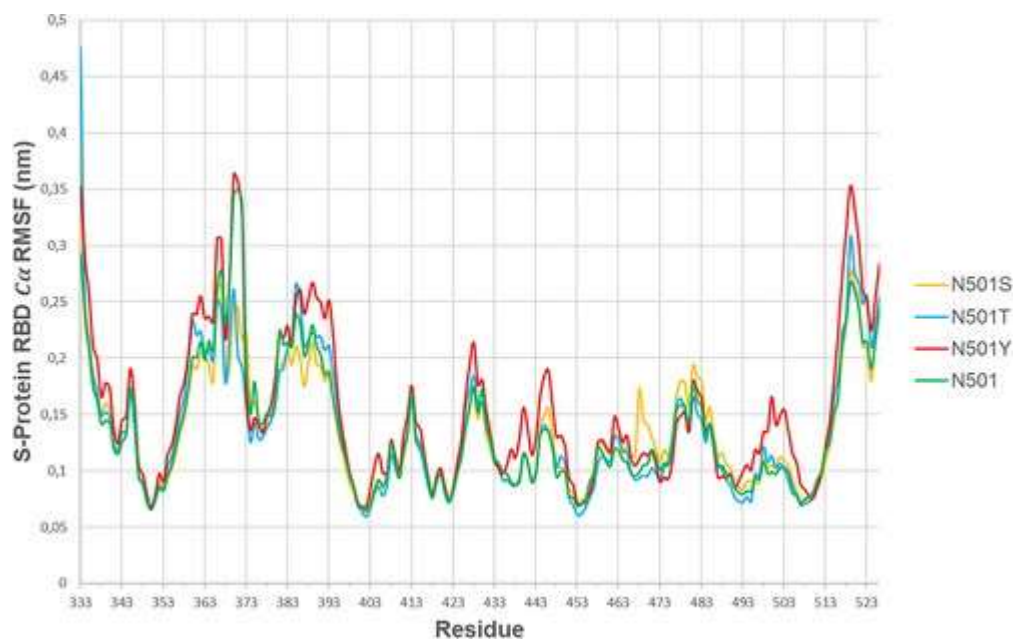
Novel and original biomolecular findings related to the consequences of N501Y mutation:

- Two S-protein variants considered: wild type (bearing N501) and mutant (bearing Y501).
- The hydrogen bond <RBD> Gly502 N-H...O=C Lys353 <hACE2> is of temporary character in N501 variant, changed to a permanent polar contact in Y501 mutant.
- Energy calculations: $E(\text{Gly502 N-H...O=C Lys353})$ in N501Y=4.816210332kcal/mol
 $E(\text{Gly502 N-H...O=C Lys353})$ in N501=3.909532232kcal/mol
- N501Y mutation favors enhanced electrostatic interaction between Tyr505 (RBD) phenolic -OH group and Glu37 (hACE2) side chain oxygen atoms.
- I prove the presence of a Y501 binding pocket, based on RBD [499-505]: PTYGVGY $\text{Ca}'\text{s}$ RMSF peak formation.



5. Related COVID-19 Research

- **Journal:** Biotechnology & Biotechnological Equipment, Taylor and Francis
- **Article:** Stojanov, D. (2023). Structural implications of SARS-CoV-2 Surface Glycoprotein N501Y mutation within receptor-binding domain [499-505]–computational analysis of the most frequent Asn501 polar uncharged amino acid mutations. Biotechnology & Biotechnological Equipment, 37(1), 2206492.



5. Related COVID-19 Research

- **Journal:** Gene & Protein in Disease
- **Article:** On the in silico application of the center-of-mass distance method

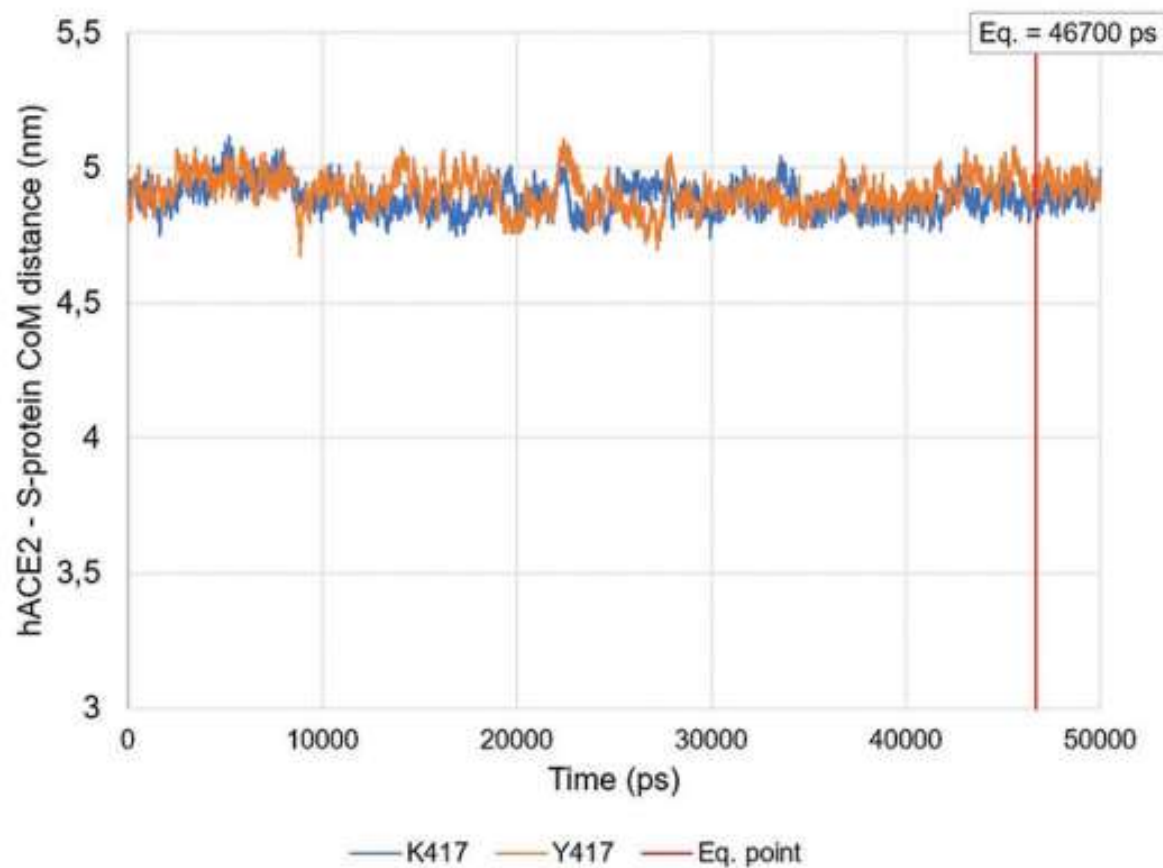
Novel in silico method for estimating binding affinity change between molecules in heterodimers, induced by one or more mutations:

- Two heterodimers considered: **W** (wild type) and **M** (mutant, a variant of W, including one or more mutations in one of the units).
- **The idea:**
 1. Simulate W and M's molecular dynamics in GROMACS and monitor CoM (Center of Mass) distance between monomers in W and M.
 2. Find the starting point of common convergence in both systems or stable CoM distance amplitudes in both systems.
 3. Apply the following rule:
 - If $M_CoM\text{-distance}(\text{during convergence}) > W_CoM\text{-distance}(\text{during convergence})$
induced mutations decrease binding affinity between monomers;
 - If $M_CoM\text{-distance}(\text{during convergence}) < W_CoM\text{-distance}(\text{during convergence})$
induced mutations increase binding affinity between monomers;
 - If $M_CoM\text{-distance}(\text{during convergence}) = W_CoM\text{-distance}(\text{during convergence})$
induced mutations have no impact on binding affinity;



5. Related COVID-19 Research

- **Journal:** Gene & Protein in Disease
- **Article:** On the in silico application of the center-of-mass distance method





Thank you!

Done Stojanov, Associate Professor PhD
done.stojanov@ugd.edu.mk

